Clinical Interventions in Aging

Dovepress
Taylor & Francis Group

Open Access Full Text Article

ORIGINAL RESEARCH

# Deep Learning-Assisted Radiomics for Predicting Thoracolumbar Osteoporotic Vertebral Fractures

Minghao Che[1,2,*], Yue Chen[1,2,*], Mohamad Noor Shafini[3], Izzad Ramli[4], Hui Yang[1], Zhen Yang[1,2], Jiang Li[1,5], Jian Qin[1,5]

[1]Department of Radiology, the second Affiliated Hospital of Shandong First Medical University, Tai'an, People's Republic of China; [2]Shandong First Medical University, Jinan, People's Republic of China; [3]Medical Imaging Department, Faculty of Health and Life Sciences, St Luke's Campus, Exeter, UK; [4]College of Computing, Informatics and Mathematics, Universiti Teknologi MARA, Shah Alam, Malaysia; [5]Centre for Medical Imaging, Faculty of Health Sciences, Universiti Teknologi MARA, Puncak Alam, Malaysia

*These authors contributed equally to this work

Correspondence: Jian Qin; Jiang Li, Department of Radiology, The Second Affiliated Hospital of Shandong First Medical University, 366 Taishan Street, Tai'an, Shandong, People's Republic of China, Email sdqinjian@126.com; siyany@163.com

Clinical Interventions in Aging downloaded from https://www.dovepress.com/
For personal use only.

**Rationale and Objectives:** Osteoporotic vertebral compression fractures (OVFs), particularly at the thoracolumbar spinal junction spanning levels T11 to L2, represent a significant and debilitating global health challenge. The objective of the present research was to establish and verify a robust radiomics model using routine non-contrast computed tomography (CT) to predict thoracolumbar OVFs risk.

**Materials and Methods:** In this retrospective cohort study, 80 patients with new thoracolumbar OVFs were propensity-matched 1:2 with 160 controls. A 3D U-Net automatically segmented T11-L2 cortical and cancellous bone. Following minimum redundancy maximum relevance (mRMR) and least absolute shrinkage and selection operator (LASSO) feature selection, 13 cortical and 16 cancellous radiomics features were extracted. Logistic regression models were developed using corresponding radscores. The best-performing model was compared to volumetric bone mineral density (vBMD) and evaluated via ROC curves, decision curve analysis (DCA), and calibration plots.

**Results:** A total of 240 patients (147 females, 93 males) were enrolled, with no significant age or sex differences between groups. The combined cortical and cancellous radscore model (vertebral model) attained an AUC of 0.825 and 0.840 for OVF prediction, outperforming the vBMD model (AUC: 0.752/0.735). DCA and calibration plots verified its outstanding predictive performance. Notably, integrating vBMD with the vertebral model did not yield a statistically significant improvement ($p > 0.05$). The selected features highlighted crucial microstructural insights, with cancellous features reflecting trabecular heterogeneity and cortical features indicating mineralization uniformity and integrity.

**Conclusion:** Our findings demonstrate that radiomics derived from routine non-contrast CT, leveraging deep learning for automated bone compartment segmentation, offers a superior and practical tool for Early identification of high-risk individuals for thoracolumbar OVFs. This approach provides valuable, complementary information beyond vBMD, potentially enhancing clinical decision-making and reducing the burden of osteoporosis.

**Keywords:** osteoporotic vertebral fractures, deep learning, radiomics, fracture prediction

## Introduction

Osteoporosis is a systemic skeletal disorder defined by diminished bone strength and elevated bone fragility, which poses a prominent challenge to global public health.[1] Its prevalence escalates with the aging population, imposing substantial socio-economic burdens and severely diminishing patients' quality of life.[2] Among the various consequences of osteoporosis, fragility fractures are the most debilitating. OVFs are the most prevalent type, impacting approximately one-third of postmenopausal women and a substantial proportion of older men.[3] The thoracolumbar junction, spanning the T11 to L2 vertebrae, represents a critical transitional zone in the human spinal column. This structure links the thoracic spine (rigid, kyphotic, and stabilized by the thoracic cavity) with the lumbar spine (more flexible and lordotic).[4]

https://doi.org/10.2147/CIA.S600030
Received: 30 January 2026
Accepted: 11 May 2026
Published: 20 May 2026



© 2026 Che et al. This work is published and licensed by Dove Medical Press Limited. The full terms of this license are available at https://www.dovepress.com/terms.php and incorporate the Creative Commons Attribution – Non Commercial (unported, v4.0) License (http://creativecommons.org/licenses/by-nc/4.0/). By accessing the work you hereby accept the Terms. Non-commercial uses of the work are permitted without any further permission from Dove Medical Press Limited, provided the work is properly attributed. For permission for commercial use of this work, please see paragraphs 4.2 and 5 of our Terms (https://www.dovepress.com/terms.php).

This region endures substantial stress during flexion, extension, and axial loading, making the T11 to L2 vertebrae the most frequent sites for vertebral fractures.[5]

The clinical reference criterion for diagnosing osteoporotic conditions and evaluating fracture susceptibility is the two-dimensional areal bone mineral density (aBMD) provided by dual-energy X-ray absorptiometry (DXA).[6] However, aBMD has significant limitations in predicting fractures, with approximately 50% of vertebral fractures occurring in individuals whose T-scores do not meet the osteoporosis criteria.[7,8] This diagnostic gap underscores the need for more sophisticated and sensitive methods to identify high-risk individuals before fractures occur. vBMD measured by quantitative computed tomography (QCT) can provide a three-dimensional assessment of bone density that is unaffected by aortic calcification or degenerative spinal changes, thus more accurately reflecting bone strength.[9,10]

Utilizing sophisticated computational algorithms, radiomics converts medical imaging scans into a high-dimensional space of quantitative data.[11] This technique deciphers pixel-level intensity, texture, and shape patterns that are invisible to the human eye.[12] In bone analysis, these radiomics features can effectively act as surrogate markers for microarchitectural integrity. Numerous studies have highlighted the potential of radiomics features in musculoskeletal applications, particularly in evaluating vertebral fragility and loading through texture analysis.[13–18] The vertebral body, however, is not homogeneous; it comprises a metabolically active trabecular core and a dense cortical shell, each contributing differently to biomechanical stability and exhibiting distinct responses to aging and metabolic diseases.[19] Most radiomics research has either treated the vertebra as a single unit or concentrated on the more easily segmented trabecular bone. Consequently, the unique predictive information in the bone cortex, which is crucial for resisting bending and torsional forces, has been largely overlooked. It remains uncertain whether cortical radiomics features offer complementary or redundant insights compared to trabecular features, and whether their integration could yield a more robust, synergistic predictive model.

This study seeks to enhance the radiomics assessment of vertebral fracture risk using routine non-contrast CT to identify individuals at high risk for OVFs early. We also Conducted a comparison of the predictive efficacy of the radiomics-based model with vBMD and assessed the efficacy of a combined model incorporating both radiomics and bone density in predicting thoracolumbar OVFs.

# Materials and Methods

## Study Population

A single-center retrospective longitudinal cohort study was performed in one hospital. The inclusion criteria encompassed: (1) a follow-up phase lasting no less than 1 year; (2) CT imaging spanning a minimum of the T11-L2 vertebral bodies was performed during the baseline period assessment. Subsequently, Any patient who fulfilled any of the predefined exclusion criteria was excluded. The exclusion criteria were as follows: (1) follow-up period shorter than 12 months; (2) inadequate imaging data availability; (3) pre-existing vertebral fragility fractures or a history of spinal surgical intervention at baseline; (4) development of trauma-related fractures or pathological fractures caused by bone metastases or osseous tumors during follow-up; (5) a past medical history encompassing endocrine disorders that disrupt calcium-phosphorus metabolism, chronic administration of pharmacotherapies impacting bone turnover, or neuromuscular conditions such as Parkinson's disease. Following up to September 2025, we included 12,638 patients in the baseline cohort. Two radiologists, blinded to clinical information, independently reviewed the CT and/or MRI images from baseline and follow-up. The diagnosis of OVFs utilizes the Genant semi-quantitative grading system alongside specific imaging indicators: (1) CT scans reveal new vertebral height loss, either wedge-shaped or biconcave, or cortical bone fracture;[20] (2) MRI T2-weighted fat-suppressed sequences show high bone marrow signal (bone marrow edema) corresponding to the area of new morphological change.[21] Any disagreements among assessors are resolved through discussion to reach a consensus. If consensus cannot be reached, the case will be referred to a more senior expert for final adjudication.

The flowchart corresponding to this study is illustrated in Figure 1.Ultimately, 80 patients who suffered newly developed fractures of the thoracolumbar vertebrae in the follow - up phase were designated as the experimental cohort (fracture cohort) and incorporated into the present experiment (Figure 2a). To control selection bias and ensure baseline comparability between groups, we applied Propensity Score Matching (PSM) using age and gender as covariates.

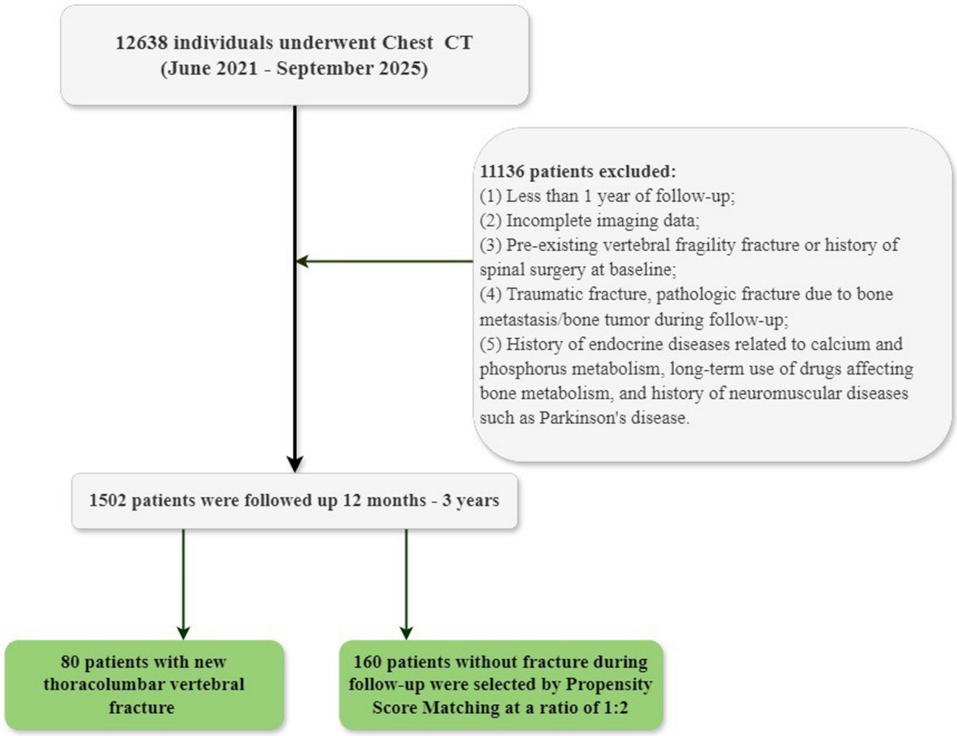


**Figure 1** Flowchart for the patient selection. CT, computed tomography.

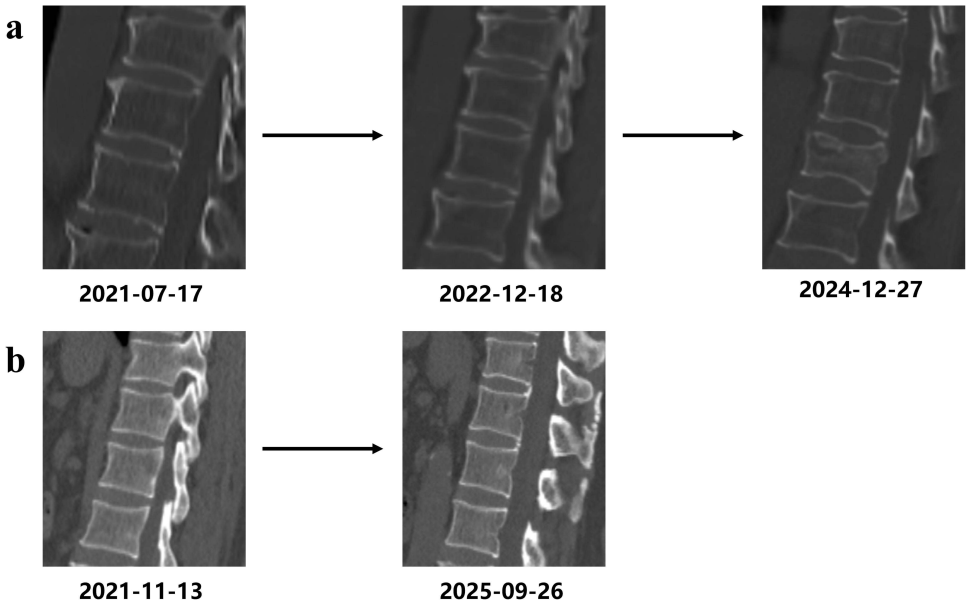


**Figure 2** Whether OVFs occurred during the follow-up. (**a**), OVFs occurred during the follow-up (T11-L2). (**b**), No OVFs occurred during the follow-up (T11 - L2).

Consequently, 160 patients who did not experience fractures during the same period were matched at a 1:2 ratio as the control group (non-fracture group) (Figure 2b). Both patient groups met identical inclusion and exclusion criteria. Ethical approval for the present research was granted by the hospital's ethics committee. As the study was of a retrospective nature, no informed consent forms were required to be signed.


https://doi.org/10.2147/CIA.S600030

## The Collection of CT Imaging Data

All subjects underwent standard non-contrast CT examinations as a screening procedure at the baseline stage. The scanning device was the 256-slice Revolution CT produced by General Electric Company of the United States. The scanning parameters were uniformly set as follows: tube voltage of 120 kV, tube current of 400 mAs, reconstruction slice thickness and slice interval both of 1.25 mm, and matrix of 512×512.

## Image Segmentation Based on 3D U-Net

The original CT thin-slice images were imported into the AW4.7 post-processing workstation (GE Company). Using the bone window settings (window width: 2000 HU, window level: 350 HU), the "reformat" function was employed to reconstruct the vertebral body images into a standard DICOM sequence with a slice thickness of 1.25 mm. The reconstructed images were then imported into the quantitative CT spine bone analysis system. This system, developed jointly by the Second Affiliated Hospital of Shandong First Medical University and Hangzhou Shimai Company (Computer Software Copyright Registration No. 2024SR0222436),[22] utilized a deep-learning-driven framework to automatically segment each vertebral body into two volumes of interest (VOIs): the vertebral body cortical bone VOI and the vertebral body cancellous bone VOI (Figure 3). Each patient had a total of 8 VOIs.

## vBMD Measurements

Mediastinal window thin-section CT scans acquired during the baseline assessment were transmitted to the professional QCT workstation. Routine calibration was performed using the QCT model manufactured by Mindways (USA). Cortical

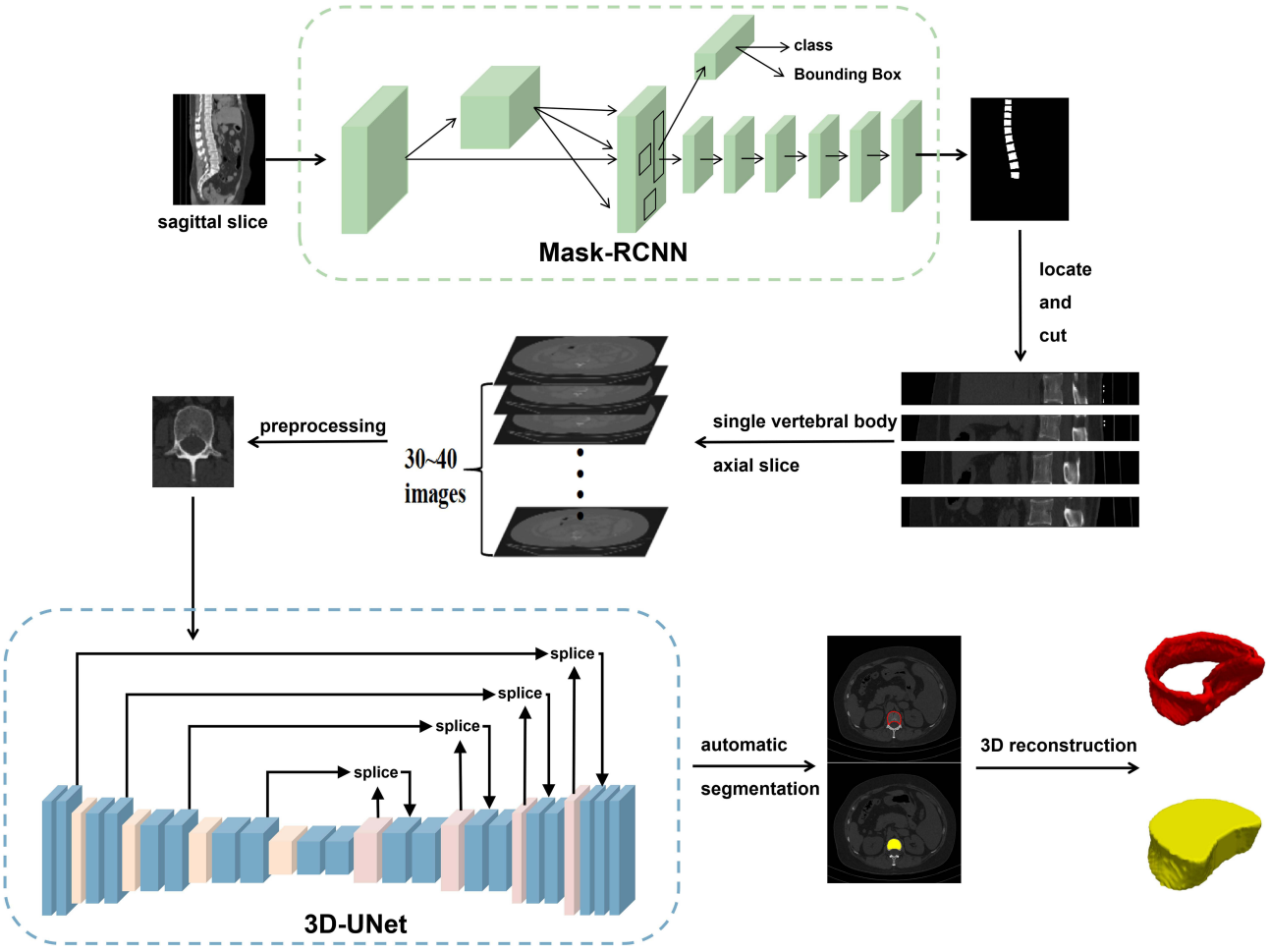


**Figure 3** Automatic vertebra segmentation based on 3D U-net deep learning algorithm.

skeletal tissue, hyperplastic osseous tissue, osseous islands, the posterior vertebral venous plexus, as well as other tissue regions with heterogeneous characteristics were excluded from the research cohort. A region of interest (ROI) with an area of 100 $mm^2$ was positioned within cancellous bone compartment of the T11-L2 vertebrae on the QCT images. The chosen ROIs were subjected to automatic analysis and processing via the QCT Professional software, so as to acquire the vBMD values (Figure 4).[23] One single scanning session was utilized to obtain two distinct thin-slice sequences: the conventional CT sequence (1.25 mm STND) and the QCT-specific sequence (1.25 mm STND), which eliminated the necessity for supplementary CT examinations or contrast medium administration.

## Radiomics Feature Extraction and Selection

Feature extraction for each VOI was performed using the Research Portal V1.1 workstation developed by United Imaging Intelligence Co., Ltd., Shanghai, PRC. To mitigate the confounding effects of CT image noise and iterative algorithms for image reconstruction on the stability of extracted radiomics features, it was necessary to conduct standardized preprocessing of the images obtained before feature extraction. Classification of The extracted radiomics feature sets was conducted into 7 major groups, namely First Order, Shape, Gray - Level Co - Occurrence Matrix (GLCM), Gray - Level Run - Length Matrix (GLRLM), Gray - Level Size Zone Matrix (GLSZM), Gray - Level Dependence Matrix (GLDM), and Neighboring Gray - Tone Difference Matrix (NGTDM). Moreover, to capture deeper texture information, multiple filters were applied to the images. Ultimately, radiomics features were extracted based on 15 transformation types in total, which included Original, BoxMean, Additive Gaussian Noise, binomialblurimage, Curvature Flow, Boxsigmalmage, LoG, Wavelet, Normalize, Laplacian Sharpening, Discrete Gaussian, Mean, Speckle Noise, Recursive Gaussian and ShotNoise.

Not all extracted features are applicable for subsequent analysis. To guarantee the comparability of data and enhance the reproducibility as well as reliability of the research findings, maximum absolute value normalization was performed on these features. Subsequently, the mRMR method was employed to further reduce the dimensionality of the data. Based on the correlations between features and their potential associations with fractures, some features with low correlations and redundancies are removed, and the top 30 most representative features are selected. Subsequently, LASSO is used. After 10 - fold cross - validation, the most valuable radiomics features related to fractures are screened at the optimized $\lambda$ point.

## Establishment and Validation of the Models

Two hundred and forty study participants were categorized into a training cohort (70%, n = 168) and a test cohort (30%, n = 72). The training cohort was utilized to build the model, and the test cohort was employed for model validation. The optimal radiomics features, selected through mRMR and LASSO regression analyses, were multiplied by their respective coefficients and subsequently summed. Given that the four vertebral bodies from T11 to L2 were considered collectively

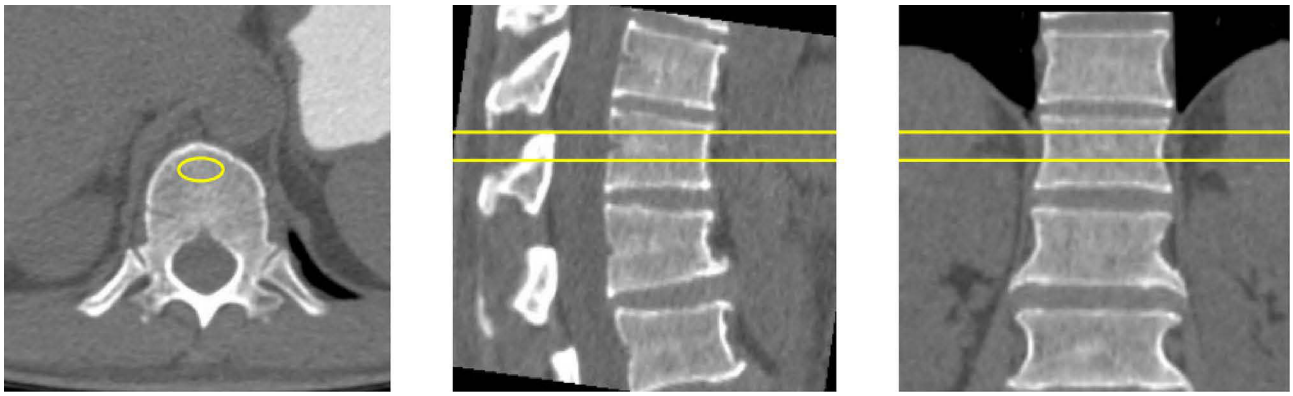

**Figure 4** Schematic diagram of measuring QCT. The yellow elliptical area represents the selected vertebral ROI in the axial image; it intersects with the yellow solid lines in the coronal and sagittal views, and together they define an elliptical cylinder VOI in three-dimensional space.
**Abbreviations**: QCT, quantitative computed tomography; ROI, region of interest; VOI, volume of interest.


https://doi.org/10.2147/CIA.S600030

in this study, the average value of these vertebral bodies was utilized as the final radscore. This score effectively reflects the association between the radiomics features of the patients' vertebral bodies and their fracture risk. Subsequently, logistic regression was utilized to establish three radscore models: cortical bone model, cancellous bone model, and their combined model (vertebral model). The diagnostic performance of these models in predicting thoracolumbar OVFs was evaluated by computing the area under the ROC curve.

The vBMD was added to The optimal-performing model among the above three models to establish a combined model. The predictive performances of the vBMD model, radscore model, and combined model for thoracolumbar OVFs were evaluated by AUC, specificity, sensitivity, accuracy, etc., we analyzed whether statistically significant differences existed between the various AUC values. To visualize the discriminative ability and calibration analysis of the three models as well as evaluate their predictive capacity, We utilized calibration plots to assess the consistency between the actual probability of fracture occurrence and the fracture probability predicted by the models. Additionally, decision curve analysis (DCA) was employed for the evaluation of the models' ability to correctly predict fractures and their clinical applicability.

## Statistical Analysis

All statistical analyses for this research were performed with the use of R version 4.4.3. The DeLong Test was employed for the comparison of the performance of the ROC curves between the two models, and $p < 0.05$ was considered statistically significant.

# Results

## Clinical Characteristics

Table 1 outlines the baseline demographics. The study comprised 80 cases of thoracolumbar vertebral fragility fractures, with an age averaging 70.86 years, including 49 females and 31 males. A control group of 160 non-fractured individuals, matched for age and gender, was randomly selected at a 1:2 ratio. The control group averaged 71.02 years, consisting of 98 females and 62 males. No significant differences in age and gender were observed between the fracture and control groups ($p > 0.05$). Notably, the fracture group exhibited a significantly lower average thoracolumbar vertebral vBMD compared to the control group (93.16 ± 16.05 mg/cm$^3$ vs. 111.75 ± 20.29 mg/cm$^3$; $p < 0.001$).

## Radiomics Feature Selection

After automatic vertebral body segmentation using the 3D U-Net deep learning-based algorithm, we extracted 2286 radiomics features from the cortical bone and cancellous bone regions respectively. For the cortical bone, dimensionality reduction using mRMR and Lasso regression identified 13 radiomics features, with the optimalλvalue at 0.037 (Figure 5a). Similarly, for the cancellous bone, dimensionality reduction yielded 16 features, with the optimalλvalue at 0.032 (Figure 5b). These features were selected for subsequent model development.

## Radscore Model Construction and Evaluation

For the cortical bone region, the 13 radiomics features were multiplied by their coefficients and then summed up. Each patient had 4 Radscores, and the average of the 4 Radscores was designated designated as the final Radscore for

**Table 1** Baseline Characteristics of the Study Population

| | Fracture (n=80) | Non-Fracture (n=160) | *P* |
|---|---|---|---|
| **Age (years)** | 70.86±8.61 | 71.02±8.79 | 0.969 |
| **Sex** | | | 1 |
| **Female** | 49 | 98 | |
| **Male** | 31 | 62 | |
| **BMI** | 22.42±2.68 | 23.79±3.81 | 0.076 |
| **VBMD** | 93.16±16.05 | 111.75±20.29 | <0.001 |

 https://doi.org/10.2147/CIA.S600030 

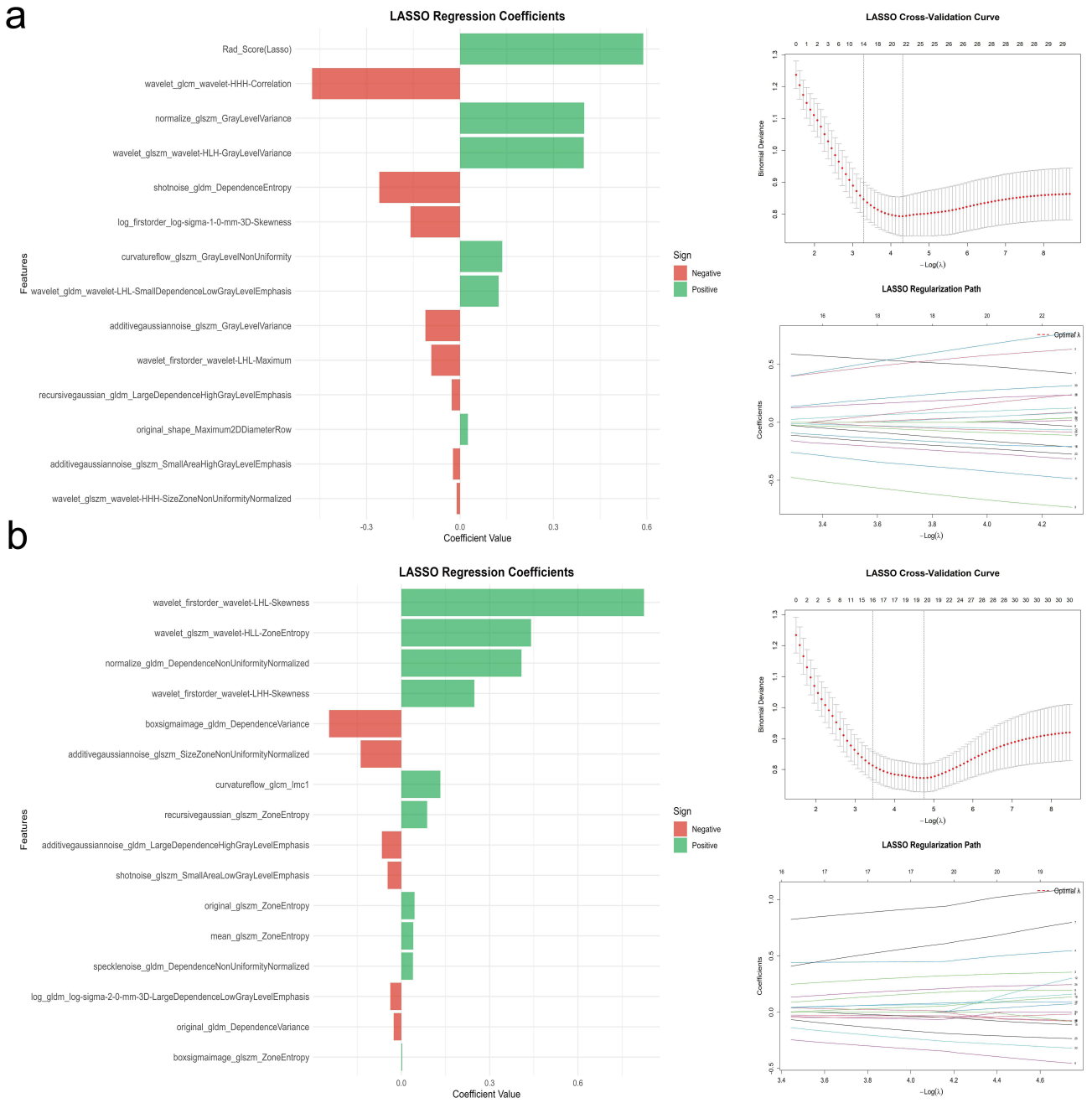


**Figure 5** Schematic of radiomics feature selection. Feature selection proceeded using mRMR and the LASSO. (**a**) LASSO regression coefficient plot, cross-validation curve, and regularization path for cortical bone. (**b**) LASSO regression coefficient plot, cross-validation curve, and regularization path for cancellous bone. The optimal λ value for the cortical bone was 0.037 (**a**). The cancellous bone selects the optimal λ value of 0.032 (**b**).
**Abbreviations**: LASSO, the least absolute shrinkage and selection operator; mRMR, minimum-Redundancy Maximum-Relevancy.

individual patients and incorporated into the logistic regression predictive model to construct a cortical bone model for assessing the risk of osteoporotic fractures in the thoracolumbar vertebrae. The formula is:

Radscore 0.3976 * wavelet_glszm_wavelet-HLH-GrayLevelVariance+
0.3990 * normalize_glszm_GrayLevelVariance+
0.0251 * original_shape_Maximum2DDiameterRow+
0.1239 * wavelet_gldm_wavelet-LHL-SmallDependenceLowGrayLevelEmphasis+
0.1353 * curvatureflow_glszm_GrayLevelNonUniformity+
-0.4752 * wavelet_glcm_wavelet-HHH-Correlation+


https://doi.org/10.2147/CIA.S600030

-0.1588 * log_firstorder_log-sigma-1-0-mm-3D-Skewness+
-0.2593 * shotnoise_gldm_DependenceEntropy+
-0.0107 * wavelet_glszm_wavelet-HHH-SizeZoneNonUniformityNormalized+
-0.0266 * recursivegaussian_gldm_LargeDependenceHighGrayLevelEmphasis+
-0.0224 * additivegaussiannoise_glszm_SmallAreaHighGrayLevelEmphasis+
-0.0920 * wavelet_firstorder_wavelet-LHL-Maximum+
-0.1111 * additivegaussiannoise_glszm_GrayLevelVariance+

For the cancellous bone region, the cancellous bone model was established through the same process. The formula is:
Radscore=0.8243 * wavelet_firstorder_wavelet-LHL-Skewness+
0.0395 * specklenoise_gldm_DependenceNonUniformityNormalized+
0.2480 * wavelet_firstorder_wavelet-LHH-Skewness+
0.4405 * wavelet_glszm_wavelet-HLL-ZoneEntropy+
0.0449 * original_glszm_ZoneEntropy+
0.4082 * normalize_gldm_DependenceNonUniformityNormalized+
0.0878 * recursivegaussian_glszm_ZoneEntropy+
0.0405 * mean_glszm_ZoneEntropy+
0.0030 * boxsigmaimage_glszm_ZoneEntropy+
0.1326 * curvatureflow_glcm_Imc1+
-0.2450 * boxsigmaimage_gldm_DependenceVariance+
-0.0257 * original_gldm_DependenceVariance+
-0.0371 * log_gldm_ LargeDependenceLowGrayLevelEmphasis+
-0.0462 * shotnoise_glszm_SmallAreaLowGrayLevelEmphasis+
-0.1381 * additivegaussiannoise_glszm_SizeZoneNonUniformityNormalized+
-0.0660 * additivegaussiannoise_gldm_LargeDependenceHighGrayLevelEmphasis

The cortical bone radscore and cancellous bone radscore were combined to evaluate the fracture risk as a vertebral model. The AUC of the cortical bone model was 0.778 and 0.776, while the AUC of the cancellous bone model was 0.808 and 0.797. The AUC of the vertebral model, which integrated cortical and cancellous bone parameters, was 0.825 and 0.840. In the testing cohort, the vertebral body model demonstrated a higher AUC compared to the cortical bone model or cancellous bone model, indicating improved performance in predicting vertebral fracture risk (Figure 6). Among the remaining Diagnostic efficiencies, except for sensitivity and negative predictive value (npv), the vertebral body model demonstrated good performance (Tables 2 and 3).

## Comparison Between the Radiomics and vBMD Models

Incorporating vBMD into the vertebral model yielded a combined model. Figure 7 illustrates the fracture prediction performance across three models. In the training cohort, the AUC values were 0.752, 0.825, and 0.841, while in the testing cohort, they were 0.735, 0.840, and 0.848, respectively. Predictive accuracy values for the vBMD, vertebral, and combined models are presented in Tables 4 and 5. DeLong Test results are provided in Table 6.

# Discussion

This study aimed to enhance the utilization of radiomics in assessing OVFs risk through conventional non-enhanced CT scanning techniques, focusing on identifying populations at high risk for OVFs in the thoracolumbar region (T11-L2). The thoracolumbar junction experiences a higher biological stress concentration due to varying vertebral body loads, with many OVFs occurring in this specific area.[24,25] By employing advanced imaging methods such as radiomics feature extraction and 3D U-Net-based automated segmentation of vertebral bodies, predictive models for OVFs were developed and assessed based on cortical and cancellous bone radiomics features individually and in combination, with a comparison made to vBMD performance. Our study suggests that the vertebral model offers additional value in fracture prediction, surpassing the predictive capability of vBMD. Notably, integrating the omics model with the vBMD model did not yield a statistically significant enhancement in predictive performance. This study underscores the

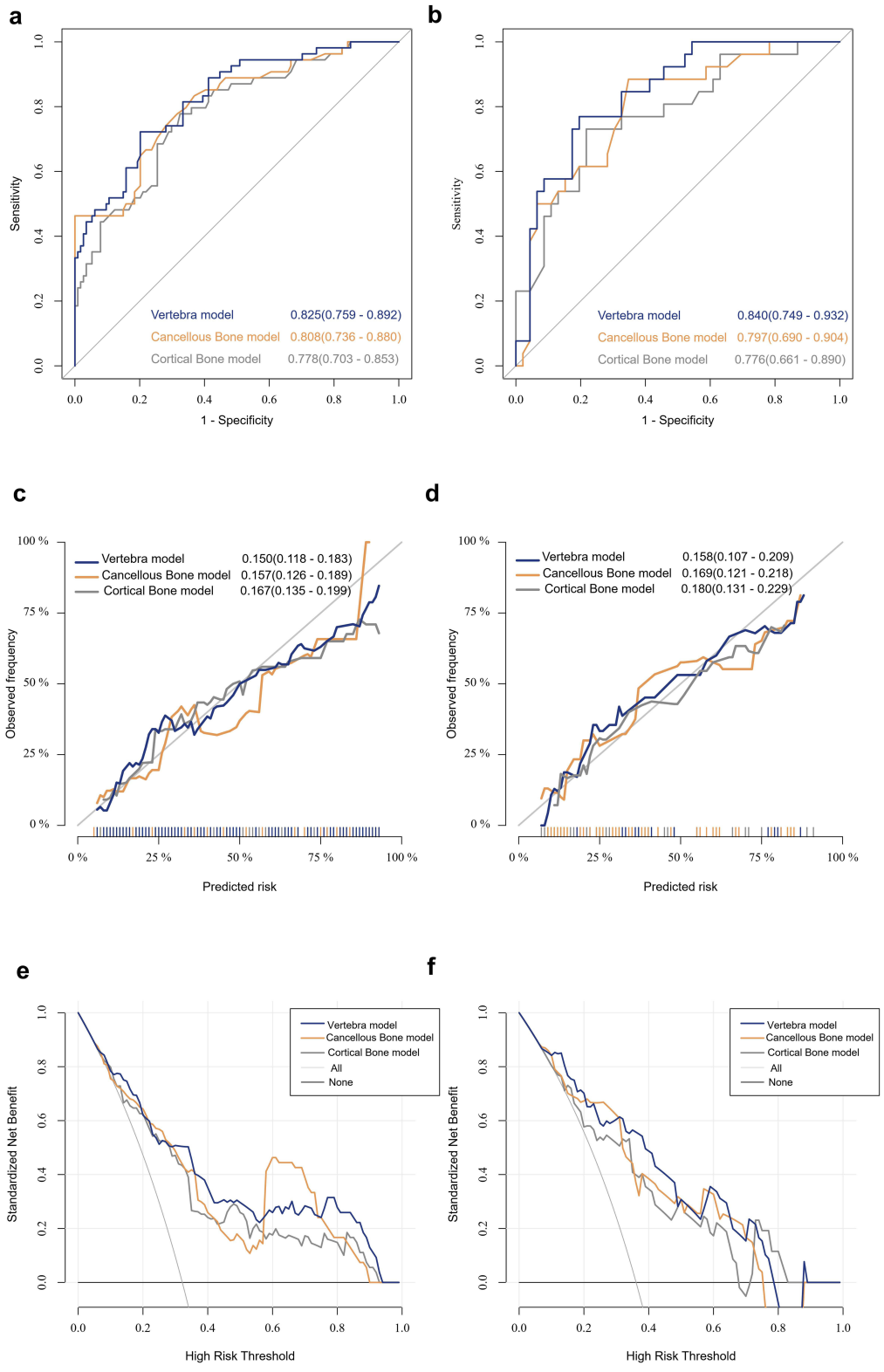


**Figure 6** Performance comparison of Cortical Bone model, Cancellous Bone model and Vertebral model. The ROC curves of three models in the training cohort (**a**) and testing cohort (**b**). The calibration plots of three models in the training cohort (**c**) and testing cohort (**d**). DCA of three models in the training cohort (**e**) and testing cohort (**f**). **Abbreviations**: ROC, Receiver operating characteristic curves; DCA, decision curve analysis.


https://doi.org/10.2147/CIA.S600030

**Table 2** Diagnostic Efficiency of Three Radscore Models in the Training Cohort

| | Accuracy | Sensitivity | Specificity | PPV | NPV |
|---|---|---|---|---|---|
| **Vertebra model** | 0.774 | 0.722 | 0.798 | 0.629 | 0.858 |
| **Cancellous Bone model** | 0.696 | 0.833 | 0.631 | 0.517 | 0.889 |
| **Cortical Bone model** | 0.708 | 0.778 | 0.675 | 0.532 | 0.865 |

**Abbreviations**: PPV, Positive Predictive Value; NPV, negative predictive value.

**Table 3** Diagnostic Efficiency of Three Radscore Models in the Testing Cohort

| | Accuracy | Sensitivity | Specificity | PPV | NPV |
|---|---|---|---|---|---|
| **Vertebra model** | 0.777 | 0.731 | 0.804 | 0.678 | 0.841 |
| **Cancellous Bone model** | 0.736 | 0.885 | 0.652 | 0.590 | 0.909 |
| **Cortical Bone model** | 0.722 | 0.730 | 0.717 | 0.593 | 0.825 |

**Abbreviations**: PPV, Positive Predictive Value; NPV, negative predictive value.

significance of radiomics models derived from conventional non-enhanced CT scans for early identification of high-risk individuals and for enhancing clinical decision-making in osteoporosis management.

Radiomics is a crucial tool in precision medical research, extracting and quantifying high-dimensional features from medical images to unveil tissue heterogeneity imperceptible to the human eye.[12] In the realm of bone research, these features accurately depict changes in bone microstructure, including trabecular connectivity, alignment direction, and cortical bone integrity.[13,26,27] This study focuses on extracting and analyzing radiomics features from cortical and cancellous bone regions to investigate distinct microstructural information for predicting OVFs. Prior research have indicated that features of the second order act as independent indicators for evaluating bone quality and the microstructure of trabecular bone.[28] In our research, in addition to fundamental morphological, first-order and second-order features, 15 higher-order features were obtained through the application of diverse filter transformations. For the cancellous bone region, the selected features mainly reflect the heterogeneity of its internal structure, gray distribution and connectivity of trabecular bone. The wavelet transform breaks down partition images into sub-bands corresponding to different frequency and orientation parameters. "H" denotes High-pass, which corresponds to higher-frequency and detailed features within the image, whereas "L" signifies Low-pass, pertaining to lower-frequency and overall features.[29] The positive coefficients of the three wavelet features suggest an increase in the disorderliness of gray areas within cancellous bone, signifying degradation and disorganization of the trabecular microstructure.[30] Furthermore, the positive coefficient for normalize_gldm_DependenceNonUniformityNormalized indicates that greater irregularity in the cancellous structure is associated with a higher fracture risk, aligning with the pathophysiological processes involving trabecular connectivity disruption and microstructural damage.[31] These findings collectively indicate a decrease in the macroscopic density of cancellous bone alongside a more heterogeneous, disordered, and less interconnected internal microstructure, consistent with prior research.

Feature selection in cortical regions emphasizes their crucial role in providing complementary information. In wavelet features, the HHH sub-band, which encompasses all high-frequency components, exhibits a negative correlation with fractures. This correlation arises because fractures compromise the continuity of trabecular bone and cortex, thereby diminishing the linear dependence of adjacent grayscale values. In addition, the negative coefficient of log_firstorder_log-sigma-1-0-mm-3D-Skewness indicates that the more gaps and low-density grooves there are, the higher the risk of fracture. These observations regarding cortical bone features are consistent with the generally accepted knowledge, and further reinforce our hypothesis that cortical bone microstructure and morphological characteristics play a pivotal role in the comprehensive evaluation of vertebral biomechanical stability, offering supplementary rather than redundant insights compared to cancellous bone features. By extracting multi-scale and multi-dimensional texture features, bone microstructure damage is elucidated across various levels, enabling a comprehensive quantification of bone quality. Integration of radiological data from cancellous and cortical bone enables a more thorough assessment of the biomechanical integrity of vertebral bodies.

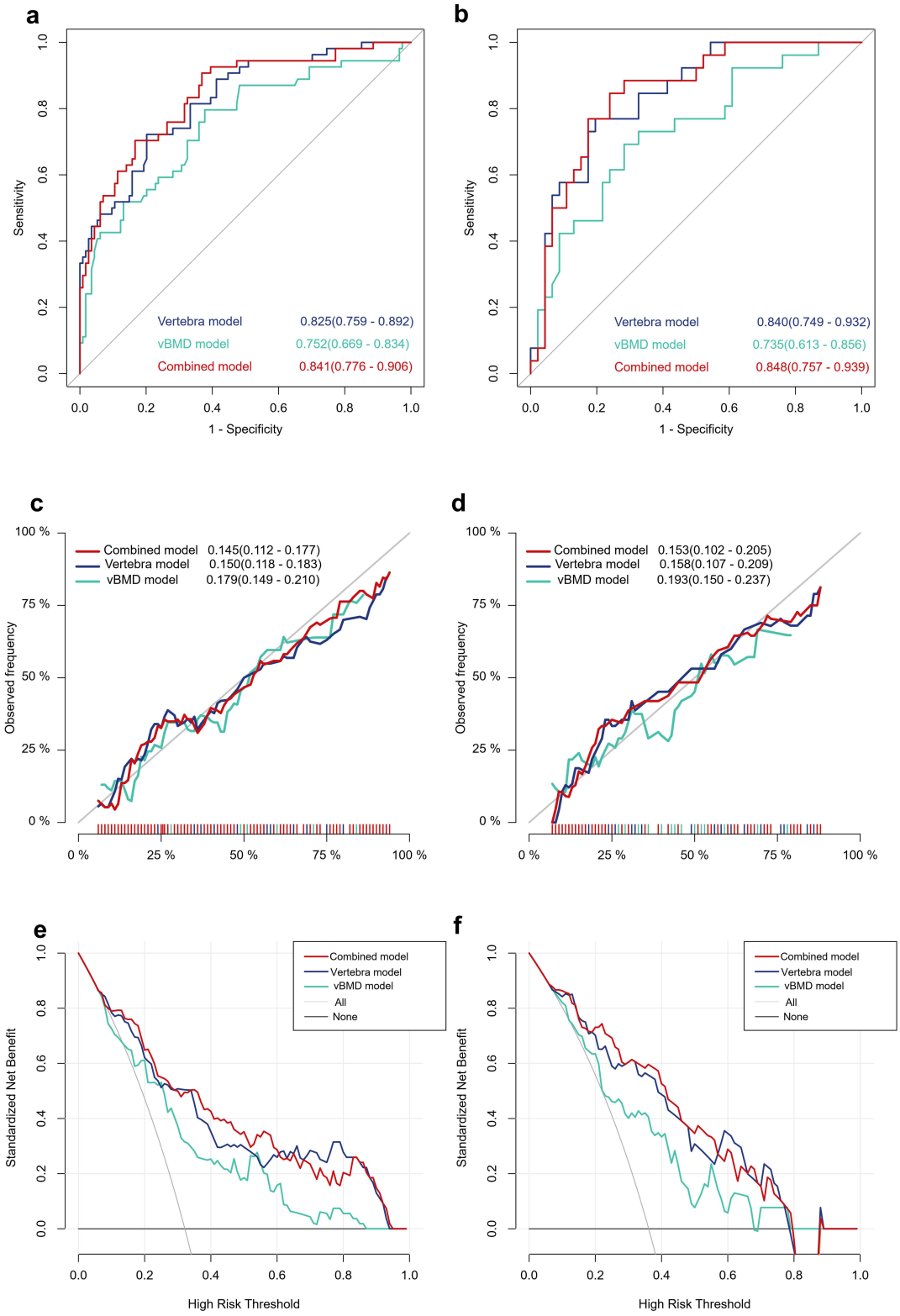


**Figure 7** Performance comparison of Vertebral model, vBMD model and Combined model. The ROC curves of three models in the training cohort (**a**) and testing cohort (**b**). The calibration plots of three models in the training cohort (**c**) and testing cohort (**d**). DCA of three models in the training cohort (**e**) and testing cohort (**f**).
**Abbreviations**: ROC, Receiver operating characteristic curves; DCA, decision curve analysis.


https://doi.org/10.2147/CIA.S600030

**Table 4** Diagnostic Efficiency of Combined, Vertebra and vBMD Models in the Training Cohort

| | Accuracy | Sensitivity | Specificity | PPV | NPV |
|---|---|---|---|---|---|
| **Combined model** | 0.720 | 0.907 | 0.631 | 0.538 | 0.935 |
| **Vertebra model** | 0.773 | 0.722 | 0.798 | 0.629 | 0.858 |
| **vBMD model** | 0.678 | 0.796 | 0.723 | 0.500 | 0.866 |

**Table 5** Diagnostic Efficiency of Combined, Vertebra and vBMD Models in the Testing Cohort

| | Accuracy | Sensitivity | Specificity | PPV | NPV |
|---|---|---|---|---|---|
| **Combined model** | 0.680 | 0.884 | 0.565 | 0.535 | 0.896 |
| **Vertebra model** | 0.778 | 0.731 | 0.804 | 0.678 | 0.841 |
| **vBMD model** | 0.597 | 0.769 | 0.500 | 0.465 | 0.793 |

**Table 6** DeLong Test Between AUCs of Combined, Vertebral, and vBMD Models

| | Training Cohort | Testing Cohort |
|---|---|---|
| **Vertebral vs Combined** | 0.13 | 0.18 |
| **Vertebral vs vBMD** | 0.05 | 0.05 |
| **Combined vs vBMD** | 0.01 | 0.04 |

Consistent with prior research, vBMD, a well-established biomarker of bone mineral content, exhibited notable distinctions between groups with and without fractures, underscoring its established predictive capacity for OVFs (AUC=0.752/0.735).[9] Nonetheless, as highlighted in the introduction, relying solely on BMD led to the oversight of a considerable number of fracture cases (accuracy of 0.68 in the training cohort and 0.60 in the test cohort). In this investigation, the vertebral model (AUC=0.825/0.840) demonstrated superior performance compared to the vBMD model. DeLong Test indicated that the addition of vBMD to the radsore model did not yield a statistically significant increase in the AUC of the combined model. Consequently, we posit that radiomics models in isolation may represent a more practical diagnostic tool for clinical use.

Currently, radiomics plays a crucial role in tumor diagnostic applications, differential diagnostic assessment, treatment response evaluation, and prognosis forecasting. Chen et al demonstrated that MRI can accurately forecast early recurrence of osteosarcoma, highlighting the predictive value of imaging techniques in tumor management scenarios.[32] Yin et al utilized radiomechanical features derived from CT and MRI scans to distinguish between sacral chordomas and giant cell tumors prior to surgery, demonstrating the applicability of radiomics in distinguishing various diseases.[33] With the advancement of research, the application of radiomics in skeletal system assessments has expanded from the analysis of bone tumors to the investigation of vertebral structure and integrity. In 2021, a radiological model was proposed for the detection of osteoporosis using T1-weighted imaging (T1WI) and T2-weighted imaging (T2WI) of the lumbar spine MRI.[34] Yang et al proved that quantitative nomograms which integrate fracture line-related clinical features and CT radiological features are capable of accurately distinguishing between acute and chronic osteoporotic vertebral compression fractures.[35] Li et al reported in 2023 that the combination of CT imaging and machine learning enables the identification of occult vertebral fractures that are not detectable via traditional diagnostic methods.[36] A recent quantitative synthesis confirmed that radiomics serves as a well-established tool for osteoporosis prediction, and radiomics models integrating CT images with deep learning algorithms exhibit enhanced diagnostic precision.[37] Although radiomics analyses have been put forward for the assessment of osteoporosis and vertebral fracture risk, there are few longitudinal studies that correlate radiomics features of the trabecular bone in thoracolumbar vertebral bodies (T11 - L2)

derived from chest CT scans with the risk of osteoporotic vertebral fractures in these vertebrae.[23,38,39] Our previous research has shown that the combination of cancellous Radscore, vBMD, and clinical features is a reliable tool for fracture assessment, but the role of cortical bone remains unexplored.[40]

In the context of a growing elderly population and escalating burden of OVFs, radiomics analysis from standard non-contrast CT scans offers a dependable means of predicting fracture risk without added radiation exposure or expense. The automated vertebral body segmentation utilizing 3D U-Net, as developed in this investigation, enhances the practicality of this approach in clinical settings. By preemptively identifying high-risk cohorts prior to fracture incidents, this methodology holds promise for enabling early interventions, reducing morbidity, and alleviating the socioeconomic repercussions of osteoporosis. Nonetheless, this study is subject to certain limitations. First, this is a single-center, retrospective study, which may limit the generality of the findings. Multi-center, diverse populations will be needed to verify the stability and reproducibility of radiomic models. Second, although 3D U-Net segmentation achieves high accuracy, manual validation is still required in some cases, indicating that automation has room for improvement. Furthermore, this study used only the logistic model and did not evaluate radiomics performance across other machine learning models, then, subsequent studies should concentrate on enlarging the size of the study cohort and evaluating various machine learning approaches.

## Conclusion

Results from this study illustrate that radiomics, derived from routine non-contrast CT scans, markedly enhances the predictive performance for OVFs. Our integrated vertebral model exhibited superior predictive performance compared to vBMD alone, by deciphering subtle microarchitectural changes in both cortical and cancellous bone. Most notably, our findings indicate that the combined imaging biomodel, which integrates radiomics features from both cortical and cancellous bone, achieved the best predictive performance. Furthermore, the integration of vBMD into this combined radiomics model did not significantly improve its predictive performance, suggesting that the extracted cortical and cancellous features independently capture sufficient microstructural degradation associated with fracture risk. This non-invasive approach offers a pragmatic and economical tool for early screening of high-risk individuals, leveraging existing clinical imaging data without additional radiation exposure. Ultimately, radiomics holds considerable promise for refining clinical decision-making and improving proactive management of osteoporosis.

## Data Sharing Statement

All data generated or analyzed during this study are not publicly available but are available from the corresponding author (Jian Qin) on reasonable request.

## Ethics Approval and Consent to Participate

Ethics approval and consent to participate Ethics committee/ IRB of The Second Affiliated Hospital of Shandong First Medical University approved this study and informed consent waiver. As this study involved the retrospective review of existing medical records, the requirement for informed patient consent was waived by the Ethics Committee. All patient data were strictly anonymized and maintained with the utmost confidentiality to protect patient privacy. Furthermore, the study was conducted in full compliance with the ethical principles outlined in the 1964 Declaration of Helsinki and its later amendments.

## Author Contributions

All authors made a significant contribution to the work reported, whether that is in the conception, study design, execution, acquisition of data, analysis and interpretation, or in all these areas; took part in drafting, revising or critically reviewing the article; gave final approval of the version to be published; have agreed on the journal to which the article has been submitted; and agree to be accountable for all aspects of the work.

## Funding

This study was supported by the National Natural Science Foundation of China (Grant 62576196), the Shandong Provincial Natural Science Foundation (ZR2024QH094).

## Disclosure

Minghao Che and Yue Chen are co-first authors for this study. The authors declare that they have no known competing financial interests or personal relationships that could have appeared to influence the work reported in this paper.

## References

1. Zeng Q, Li N, Wang Q, et al. The prevalence of osteoporosis in china, a nationwide, multicenter dxa survey. *J Bone Miner Res*. 2019;34(10):1789–1797. doi:10.1002/jbmr.3757
2. Clynes MA, Harvey NC, Curtis EM, et al. The epidemiology of osteoporosis. *Br Med Bull*.;133(1):105–117. doi:10.1093/bmb/ldaa005
3. Chou R. Low Back Pain. *Ann Intern Med*. 2021;174(8):ITC113–ITC128. doi:10.7326/AITC202108170
4. Wei Y, Tian W, Zhang GL, et al. Thoracolumbar kyphosis is associated with compressive vertebral fracture in postmenopausal women. *Osteoporos Int*. 2017;28(6):1925–1929. doi:10.1007/s00198-017-3971-x
5. Wood KB, Li W, Lebl DR, et al. Management of thoracolumbar spine fractures. *Spine J*. 2014;14(1):145–164. doi:10.1016/j.spinee.2012.10.041
6. Compston JE, McClung MR, Leslie WD. Osteoporosis. *Lancet*, 393 10169 364–376 doi: 10.1016/S0140-6736(18)32112-3.
7. Cranney A, Jamal SA, Tsang JF, et al. Low bone mineral density and fracture burden in postmenopausal women. *CMAJ*. 2007;177(6):575–580. doi:10.1503/cmaj.070234
8. Schuit SC, van der Klift M, Weel AE, et al. Fracture incidence and association with bone mineral density in elderly men and women: the Rotterdam Study. *Bone*. 2004;34(1):195–202. doi:10.1016/j.bone.2003.10.001
9. Mao SS, Li D, Syed YS, et al. Thoracic Quantitative Computed Tomography (QCT) can sensitively monitor bone mineral metabolism: comparison of thoracic qct vs lumbar qct and dual-energy x-ray absorptiometry in detection of age-relative change in bone mineral density. *Acad Radiol*. 2017;24(12):1582–1587. doi:10.1016/j.acra.2017.06.013
10. Johannesdottir F, Allaire B, Kopperdahl DL, et al. Bone density and strength from thoracic and lumbar CT scans both predict incident vertebral fractures independently of fracture location. *Osteoporos Int*. 2021;32(2):261–269. doi:10.1007/s00198-020-05528-4
11. Lambin P, Leijenaar RTH, Deist TM, et al. Radiomics: the bridge between medical imaging and personalized medicine. *Nat Rev Clin Oncol*. 2017;14(12):749–762. doi:10.1038/nrclinonc.2017.141
12. Mayerhoefer ME, Materka A, Langs G, et al. Introduction to Radiomics. *J Nucl Med*. 2020;61(4):488–495.PMID: 32060219; PMCID: PMC9374044. doi:10.2967/jnumed.118.222893
13. Levi R, Garoli F, Battaglia M, et al. CT-based radiomics can identify physiological modifications of bone structure related to subjects' age and sex. *Radiol Med*. 2023;128(6):744–754. doi:10.1007/s11547-023-01641-6
14. Wang M, Chen X, Cui W, et al. A Computed tomography-based radiomics nomogram for predicting osteoporotic vertebral fractures: a longitudinal study. *J Clin Endocrinol Metab*. 2023;108(6):e283–e294. doi:10.1210/clinem/dgac722
15. Jiang YW, Xu XJ, Wang R, et al. Radiomics analysis based on lumbar spine CT to detect osteoporosis. *Eur Radiol*. 2022;32(11):8019–8026. doi:10.1007/s00330-022-08805-4
16. Poullain F, Champsaur P, Pauly V, et al. Vertebral trabecular bone texture analysis in opportunistic MRI and CT scan can distinguish patients with and without osteoporotic vertebral fracture: a preliminary study. *Eur J Radiol*. 2023;158:110642. doi:10.1016/j.ejrad.2022.110642
17. Zhang H, Yuan G, Wang C, et al. Differentiation of benign versus malignant indistinguishable vertebral compression fractures by different machine learning with MRI-based radiomic features. *Eur Radiol*. 2023;33(7):5069–5076. doi:10.1007/s00330-023-09678-x
18. Kim Y, Kim YG, Park JW, et al. A CT-based deep learning model for predicting subsequent fracture risk in patients with hip fracture. *Radiology*. 2024;310(1):e230614. doi:10.1148/radiol.230614
19. Shahnazari M, Yao W, Wang B, et al. Differential maintenance of cortical and cancellous bone strength following discontinuation of bone-active agents. *J Bone Miner Res*. 2011;26(3):569–581. doi:10.1002/jbmr.249
20. Chen R, Zhang P, Li K, et al. Risk factors of costal pain of thoracic osteoporotic vertebral compression fractures: a multicenter retrospective analysis. *Sci Rep*. 2025;15(1):10739. doi:10.1038/s41598-025-88920-6
21. Lin J, Yang Y, Fei Q, et al. Validation of three tools for identifying painful new osteoporotic vertebral fractures in older Chinese men: bone mineral density, Osteoporosis Self-Assessment Tool for Asians, and fracture risk assessment tool. *Clin Interv Aging*. 2016;11:461–469. doi:10.2147/CIA.S101078
22. Li Y, Yao Q, Yu H, et al. Automated segmentation of vertebral cortex with 3D U-Net-based deep convolutional neural network. *Front Bioeng Biotechnol*. 2022;10:996723. doi:10.3389/fbioe.2022.996723
23. Wang S, Tong X, Fan Y, et al. Combining deep learning and radiomics for automated, objective, comprehensive bone mineral density assessment from low-dose chest computed tomography. *Acad Radiol*. 2024;31(3):1180–1188. doi:10.1016/j.acra.2023.08.030
24. Liu CJ, Zhu ZQ, Wang KF, et al. Radiological analysis of Thoracolumbar Junctional degenerative kyphosis in patients with lumbar degenerative kyphosis. *Chin Med J*. 2017;130(21):2535–2540. doi:10.4103/0366-6999.217090
25. Guo R, Li B, Zeng Z, et al. Thoracolumbar kyphosis in postmenopausal osteoporosis patients without vertebral compression fractures. *Ann Transl Med*. 2022;10(2):52. doi:10.21037/atm-21-6285
26. Pan Y, Wan Y, Wang Y, et al. Conventional chest computed tomography-based radiomics for predicting the risk of thoracolumbar osteoporotic vertebral fractures. *Osteoporos Int*. 2025;36(5):893–905. doi:10.1007/s00198-024-07338-4
27. Lu W, Huang J, Zhang Z, et al. Global hotspots and prospective trends for chondrocyte metabolic changes and oxidative stress in osteoarthritis: a bibliometric analysis. *Adv Redox Res*. 2025;15:100130. doi:10.1016/j.arres.2025.100130
28. Valentinitsch A, Trebeschi S, Kaesmacher J, et al. Opportunistic osteoporosis screening in multi-detector CT images via local classification of textures. *Osteoporos Int*. 2019;30(6):1275–1285. doi:10.1007/s00198-019-04910-1

29. Hosseini SA, Shiri I, Ghaffarian P, et al. The effect of harmonization on the variability of PET radiomic features extracted using various segmentation methods. *Ann Nucl Med*. 2024;38(7):493–507. doi:10.1007/s12149-024-01923-7
30. Müller R, Rüegsegger P. Analysis of mechanical properties of cancellous bone under conditions of simulated bone atrophy. *J Biomech*. 1996;29 (8):1053–1060. doi:10.1016/0021-9290(96)00006-1
31. Putman MS, Greenblatt LB, Sicilian L, et al. Young adults with cystic fibrosis have altered trabecular microstructure by ITS-based morphological analysis. *Osteoporos Int*. 2016;27(8):2497–2505. doi:10.1007/s00198-016-3557-z
32. Chen H, Liu J, Cheng Z, et al. Development and external validation of an MRI-based radiomics nomogram for pretreatment prediction for early relapse in osteosarcoma: a retrospective multicenter study. *Eur J Radiol*. 2020;129:109066. doi:10.1016/j.ejrad.2020.109066
33. Yin P, Mao N, Wang S, et al. Clinical-radiomics nomograms for pre-operative differentiation of sacral chordoma and sacral giant cell tumor based on 3D computed tomography and multiparametric magnetic resonance imaging. *Br J Radiol*. 2019;92(1101):20190155. doi:10.1259/bjr.20190155
34. He L, Liu Z, Liu C, et al. Radiomics based on lumbar spine magnetic resonance imaging to detect osteoporosis. *Acad Radiol*. 2021;28(6):e165–e171. doi:10.1016/j.acra.2020.03.046
35. Yang H, Yan S, Li J, et al. Prediction of acute versus chronic osteoporotic vertebral fracture using radiomics-clinical model on CT. *Eur J Radiol*. 2022;149:110197.35. doi:10.1016/j.ejrad.2022.110197
36. Li WG, Zeng R, Lu Y, et al. The value of radiomics-based CT combined with machine learning in the diagnosis of occult vertebral fractures. *BMC Musculoskelet Disord*. 2023;24(1):819.36. doi:10.1186/s12891-023-06939-0
37. Chen J, Liu S, Lin Y, et al. The quality and accuracy of radiomics model in diagnosing osteoporosis: a systematic review and meta-analysis. *Acad Radiol*. 2025;32(5):2863–2875.37. doi:10.1016/j.acra.2024.11.065
38. Li Y, Liu S, Zhang Y, et al. Deep learning-enhanced opportunistic osteoporosis screening in ultralow-voltage (80 kV) chest CT: a preliminary study. *Acad Radiol*. 2025;S1076–6332(24)00937–1.
39. Li S, Huang J, Shang T, et al. α-Ketoglutarate protects against cartilage damage via epigenetically driven metabolic reprogramming in osteoarthritis models. *J Clin Invest*. 2026;136(5):e172380. doi:10.1172/JCI172380
40. Chen Y, Che M, Yang H, et al. Predicting thoracolumbar vertebral osteoporotic fractures: value assessment of chest ct-based machine learning. *Acad Radiol*. 2025;32(10):5987–5999. doi:10.1016/j.acra.2025.06.023

**Clinical Interventions in Aging**

**Dovepress**
Taylor & Francis Group

**Publish your work in this journal**

Clinical Interventions in Aging is an international, peer-reviewed journal focusing on evidence-based reports on the value or lack thereof of treatments intended to prevent or delay the onset of maladaptive correlates of aging in human beings. This journal is indexed on PubMed Central, MedLine, CAS, Scopus and the Elsevier Bibliographic databases. The manuscript management system is completely online and includes a very quick and fair peer-review system, which is all easy to use. Visit http://www.dovepress.com/testimonials.php to read real quotes from published authors.

**Submit your manuscript here:** https://www.dovepress.com/clinical-interventions-in-aging-journal